Results

HepG2 cells were exposed to 2, 5 and 10 Gy of X-rays to determine whether deletions of mtDNA were dose dependent. Sequencing confirmed that a 161-bp fragment amplified using the F1-R1 primer set was derived from CD in this study. As shown in Figure 2, CD was detected 72 h after irradiation by X-rays at 5 and 10 Gy but not at 2 Gy by PCR using the F1-R1 primer set. Since the amount of CD formed was not dependent on the dose, thereafter we fixed the irradiation at 5 Gy for further experiments with X-rays in the current study.

To confirm whether PCR products using the F1-R1 primer set were from target sequences or not, real-time PCR products were electorphoresed in a polyacrylamide gel (Figure 3). The band from CD was induced by irradiation, but 10 days after irradiation it became undetectable.

In order to investigate the temporal pattern of CD occurrence in total mtDNA and nuclear DNA after exposure to 5 Gy of X-rays, we performed real-time quantitative PCR to measure the copy number of CD and total mtDNA per cell, normalized by PCR fragments from the nuclear β-actin gene. As shown in Figure 4, the copy number of CD reached a maximum from 24–48 h after exposure to 5 Gy of X-rays, and then decreased sharply. Assuming that the number of CD at the peak mostly reflects the induction of CD, maximal relative copy number of CD was between 1 out of 7000 (HepG2-A at 24 h) and 25,000 (HepG2 at 24 h) total mitochondrial DNA. CD was nearly undetectable 10 days after the exposure in all the cell lines examined. The copy number of total mtDNA per cell also increased 24 h after irradiation and recovered to basal levels after 45 days. During this period the copy number of mtDNA was not constant but fluctuated with different patterns amongst the cell lines studied.

The amount of mitochondria in a HepG2 cell was determined by the intensity of fluorescence after staining with Mitotracker. Exposure to X-rays increased the fluorescence intensity evenly as a whole (Figure 5). Total mitochondrial mass was calculated by 'mean intensity × area'. Compared to non-irradiated cells, mitochondrial mass increased by 3.2-fold 24 h after X-ray irradiation. The value of this increase was close to the increase of mtDNA copy number (4.4-fold). In order to determine why CD disappeared 72 h after exposure, we separated viable/surviving cells from dying/dead cells using a cell sorter 24 h after exposure to X-rays and stained with Annexin V and propidium iodide. We found that CD was only detected in the dying/dead cells but not in viable/surviving cells (Figure 6).

Because the frequency of homologous sequences in mtDNA is high, at first we had tried several pairs of primers for PCR, including nested PCR to amplify only CD specific sequences. Using the primer set reported by Kubota et al. (1997), we noticed that one of the PCR products appeared only after irradiation and sequencing revealed it to be a novel 4934-bp

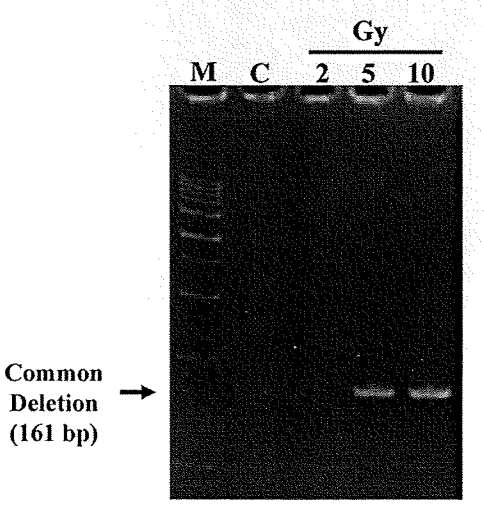

Figure 2. Profile of PCR products using primer set F1-R1 (Figure 1). Common deletion was detected 72 h after exposure of HepG2 cells to 5 and 10 Gy of X-rays but not detectable at an exposure of 2 Gy. C: without irradiation. M: 100-bp marker.

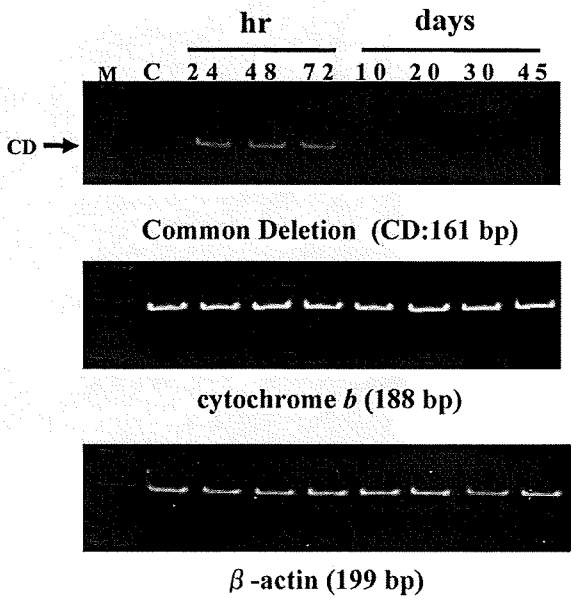

Figure 3. Electrophoretic pattern of real-time PCR products after HepG2 cells were exposed to 5 Gy of X-rays. A pair of primer set, F1-R1 in Figure 1, was used to detect common deletion (CD). CD is apparent at 72 h but not detectable 10 days after exposure. The band from cytochrome *b* represents the copy number of total mitochondrial DNA and the β-actin band that of nuclear DNA. C: without irradiation, M: 100-bp marker.

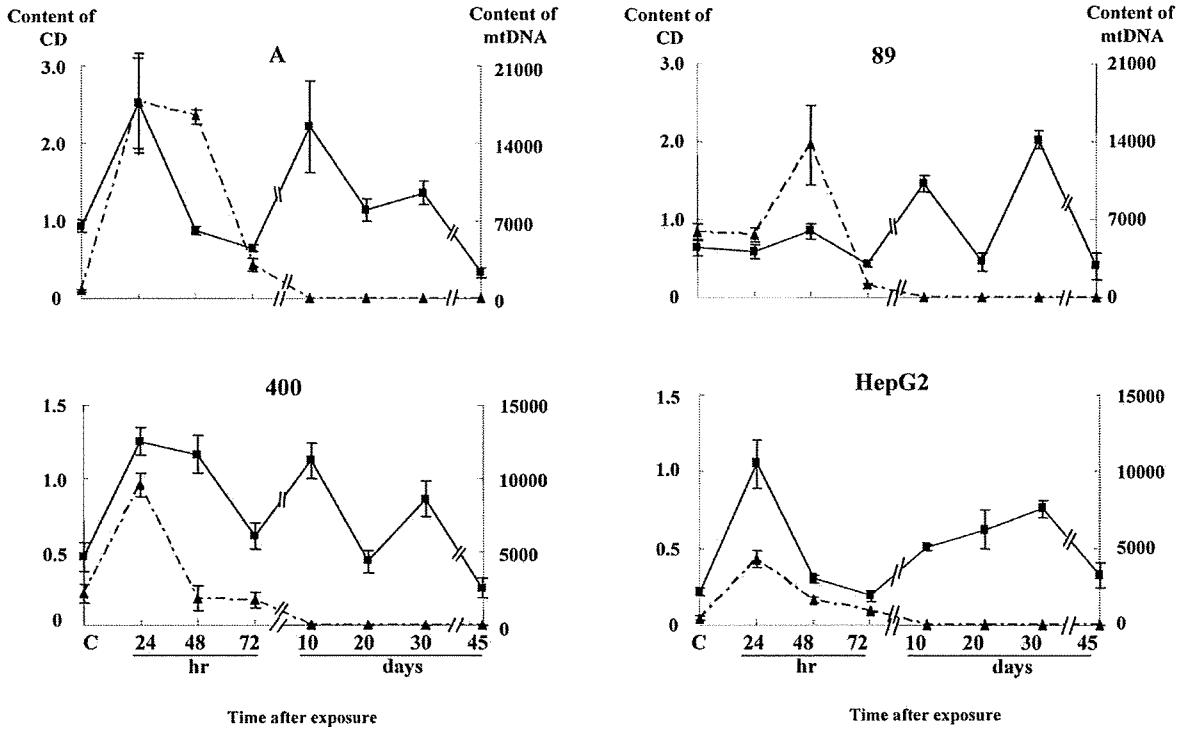

Figure 4. Temporal fluctuation profile of common deletion (▲) and total mitochondrial DNA (■). Copy number of common deletion (CD, left scale) and total mitochondrial DNA (mtDNA, right scale) was respectively normalized to that of the nuclear β-actin gene after real-time PCR. C: without irradiation. Data are means $\pm$ SD of triplicate in each experimental sample.

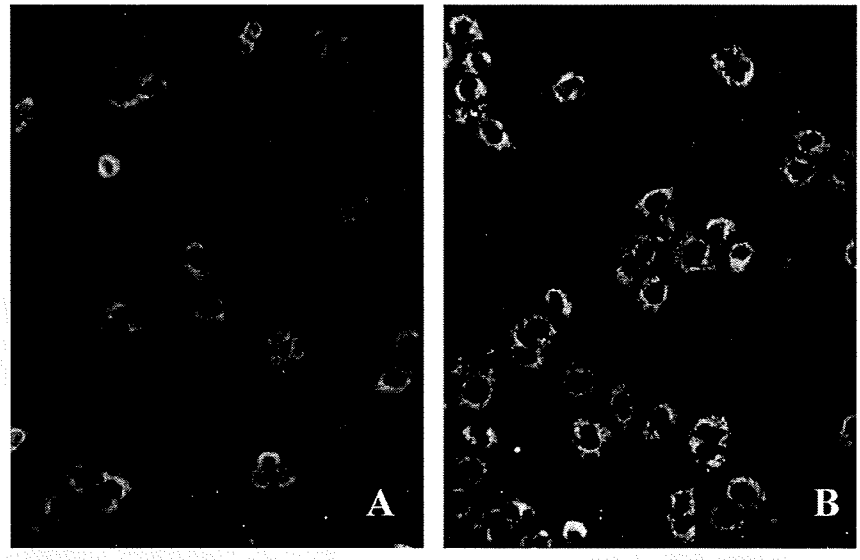

Figure 5. Mitochondria of HepG2 cells stained with Mitotracker. Compared with non-irradiated cells (A), the intensity as a whole increased 24 h after exposure to 5 Gy of X-rays (B). Original magnification: 20×.

deletion between nt8435 and nt13,368 (4934del) of mtDNA, and the 3 first deleted sequences were 'ACC' (Figure 1). This 4934del, to our knowledge, has not been previously reported. To amplify this novel 4934del effectively, we designed a new primer set, Fnd and Rnd. Primer Fnd overlays the breakpoint of 4934del but outside this novel deletion (Figure 1). Using the Fnd-Rnd primer set, 4934del

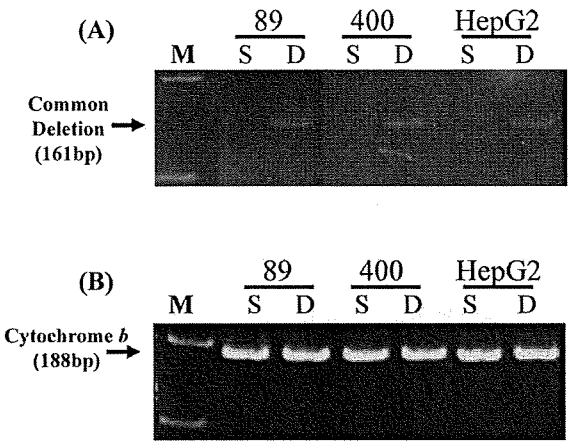

Figure 6. Detection of common deletion (CD) in dying/dead cells (D) but not in viable/surviving cells (S). Viable/Surviving cells (S) and dying/dead cells (D) were separated by a cell sorter 24 h after the cells were exposed to 5 Gy of X-rays. A primer set, F1-R1, was used to detect common deletion (CD) and cytochrome *b* to show total mitochondrial DNA. M: 100-bp marker.

was observed from 24 h after irradiation of 5 Gy X-rays to HepG2 cells and maintenance irradiation at 0.5 Gy to long-term exposed cell lines (Figure 7A). We performed real-time PCR to measure the copy number of 4934del per cell in HepG2 cells after exposure to X-rays. The copy number of 4934del before irradiation was negligible and increased up to 72 h after exposure. The copy number decreased thereafter but was detectable at a constant level (Figure 7B). This 4934del also appeared in HepG2 cells 24 h after exposure to gamma rays, alpha particles and neutrons (Figure 8A). The 4934del was not induced in HepG2 cells from 24 h to 45 days after treatment with 200 μM H_2O_2, 24–72 h after treatment with 5 μg/ml bleomycin (Figure 8B) or other anti-cancer drugs examined (data not shown).

Discussion

We could not detect CD 72 h after HepG2 cells were exposed to 2 Gy of X-rays and no apparent difference in the amount of CD induced was observed between 5 and 10 Gy-exposures. These observations suggest that a threshold dose exists for the induction of CD, but the amount of CD induced is not dependent on dose.

We found the dramatic increase in copy number for both total mtDNA and CD 24–72 h after exposure to X-rays. This indicates that CD formation is associated with the mtDNA replication induced by the preceding genetic insults by radiation, and that radiation induces over-replication of mtDNA. Basal levels of mtDNA were 2- to 3-fold higher in long-term irradiated cells compared with their parental HepG2 cells. These results suggest that a higher amount of mtDNA than that contained by HepG2 cells is needed to tolerate twice daily exposure to X-rays at a level of 0.5 Gy and that this is not enough to act as an inducible stimulus for CD. In this study, our calculation revealed that the maximum occurrence of CD corresponds to 1 out of 7000 to 25,000 copies of mitochondrial DNA. Although this occurrence of CD was insufficient to cause mitochondrial dysfunction, all traces of CD disappeared 10 days after irradiation. Therefore, we thought that mitochondria with CD were segregated into certain fractions of the cells.

In some instances, the mutated mtDNA coexists with wild-type mtDNA in a living cell (heteroplasmy) because mtDNA is present in multiple copies within a cell and wild type mtDNA can compensate for the mutated mtDNA (Morales et al. 2003). In the present study the maximum occurrence of CD was 5 copies per cell, CD was detectable only in dying cells but not at all in surviving cells. Brief treatment of cybrids containing CD mtDNA with H_2O_2 initiates a vicious cycle of mitochondrial reactive oxygen species (ROS) production resulting in apoptosis (Jou et al. 2005, Schoeler et al. 2005). Therefore, we thought that mitochondria with CD were segregated into certain fractions of the cells, and X-ray do not induce CD in all cells but only in a class of X-ray sensitive cells that are promptly eliminated by apoptosis. Characterization of cells that are prone to CD accumulation will help individualized radioprotection.

CD is reportedly induced by receiving genetic insults including ionizing radiation. Kubota et al. (1997) reported that minimal doses required for detecting CD range from 1–10 Gy of X-rays, dependent on the radiosensitivity of the cells exposed. Prithivirajsingh et al. (2004) reported that significant levels of CD accumulate 72 h after irradiation of all the human cells studied *in vitro* but they could not find a dose-response relationship or any clear relationship between sensitivity to radiation-induced deletion and sensitivity to cell death caused by radiation. In the present study, we determined the fluctuation profile of the copy number and deletions of mtDNA and showed that the total amount of CD detected in a cell population is the sum of CD induced and eliminated by cell death. Although cumulative doses for long-term irradiated cells were extraordinary high, the maintenance dose (0.5 Gy/exposure) sustained a low but variable CD copy number. Considering that cells with CD were eliminated by cell death, it would be interesting to investigate the contribution of mtDNA deletions to sub-lethal damage repair and the adaptive response.

It has been demonstrated that one of the mechanisms that produces mtDNA deletions is the pairing

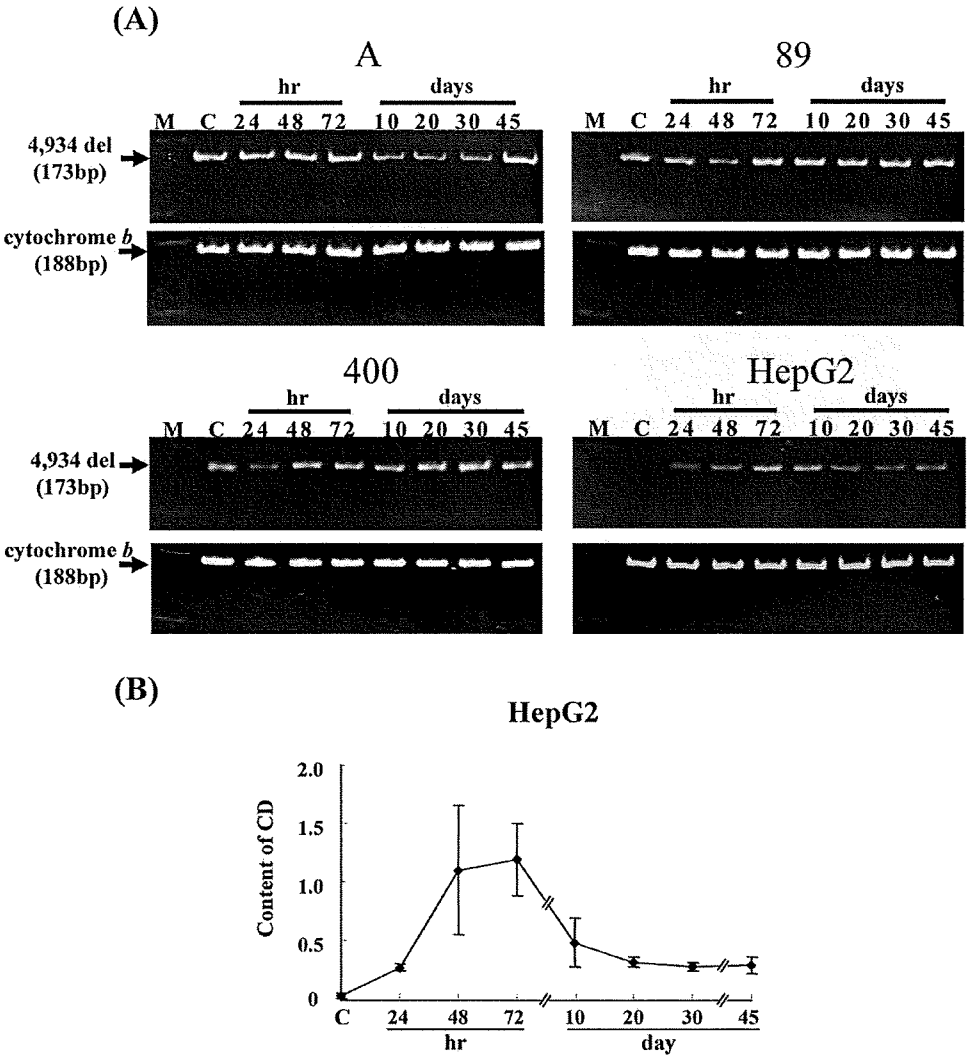

Figure 7. (A) Temporal fluctuation profile of a novel deletion (4934del) found in this study. A pair of primer set, Fnd-Rnd in Figure 1, was used to detect 4934del. 4934del was clearly induced shortly after HepG2 cells were exposed to 5 Gy of X-rays and was sustained for at least 45 days after irradiation including other sub-cell lines. (B) The change in 4934del copy number compared with that for a nuclear gene fragment in HepG2 cells exposed to X-rays at a dose of 5 Gy. Data are means ± SD of triplicate in each experimental sample. C: non-irradiated HepG2 cells and other long-term irradiated cells only, with maintenance exposure to 0.5 Gy of X-rays. M: 100-bp marker.

between two direct repeats separated by an intervening DNA fragment. Slipped-strand mispairing (SSM) is performed by non-homologous end-joining molecules which are isolated in the mitochondrial fraction of the cell (Coffey et al. 1999, Lakshmipathy & Campbell 1999). CD may arise from recombination or slippage between 13-nucleotide sequence repeats (at nt8470–8482 and nt13,447–13,459) during replication (Holt et al. 1989, Schon et al. 1989). The ends of 4934del were not related to a direct repeat but resided close to the break points of CD and the first 3-nucleotide sequence of the deleted part was ACC, which is common in CD. Both CD and 4934del were formed after irradiation, indicating that direct repeats play only a minor role in generating mtDNA deletions. This is consistent with the previous report that the vast majority of break points of different mtDNA deletions are close to the break points of CD, suggesting a common mechanism related to mtDNA replication (Samuels et al. 2004). We also found a mtDNA deletion whose 3′ end was adjacent to the sequence 'ACC' (nt13,304) after exposure to X-rays (data not shown). These results suggest the triplet sequence 'ACC' is crucial to form mtDNA deletions upon exposure to ionizing radiation. At 10 days after X-ray irradiation, CD disappeared due to the death of cells containing CD and thereafter several other PCR

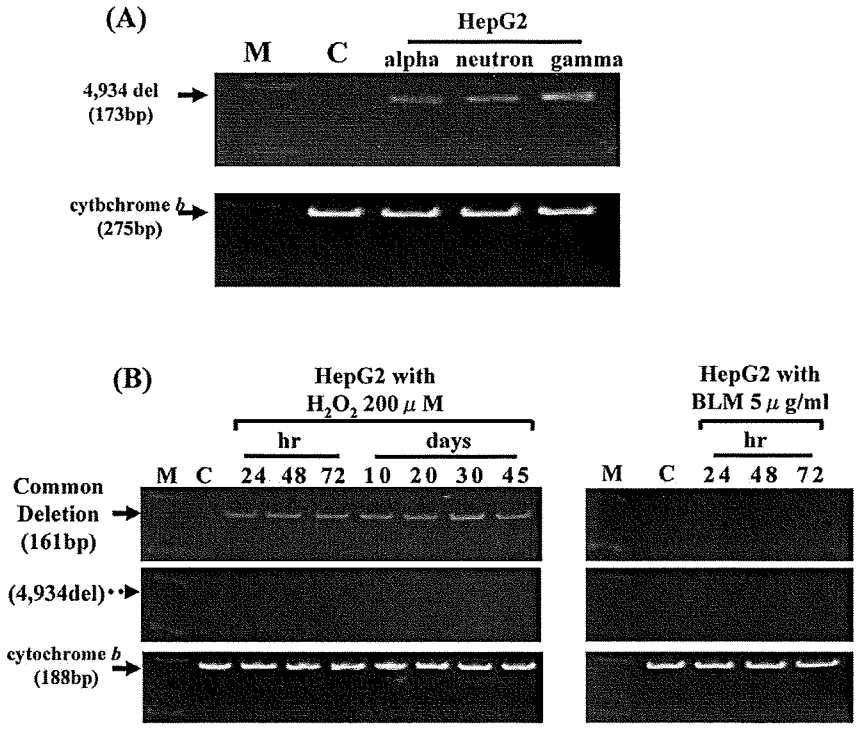

Figure 8. Association of a novel deletion, 4934del with radiation exposure. A novel deletion, 4934del that study showed was detectable 24 h after exposure to different qualities of ionizing radiation (A). 4934del was not induced in HepG2 cells by H_2O_2 treatment whereas common deletion (CD) was. Bleomycin did not induce either 4934del or CD (B). C: without irradiation. M: 100-bp marker.

products were observed using primers to detect CD partly because of abundant homologous sequences in mtDNA.

Since CD induced by UV is diminished by scavengers of ROS, this indicates that CD formation is closely linked to ROS (Berneburg et al. 1999). Bleomycin induces DNA double strand breaks via free radicals. Etoposide inhibits DNA synthesis by blocking re-ligation of DNA cleaved by topoisomerase II. 5-FU acts as a pyrimidine antagonist. Vincristine acts as an antimicrotubule agent that blocks mitosis by arresting cells in the metaphase (Ratain 2001). All the anticancer agents except vincristine used in this study are genotoxic. This is especially true for bleomycin, which is generally regarded as a radiomimetic agent because it efficiently induces DNA double strand breaks and chromatid breaks (Adema et al. 2003). In this study, CD was induced by H_2O_2 treatment and irradiation, whereas 4934del was induced by irradiation but not by H_2O_2 or other anti-cancer reagents. In addition, we did not find 4934del either in brain tissues diagnosed with Alzheimer's disease or in normal brain tissues from elder persons (data not shown). Furthermore, 4934del was clearly observed in all the cell lines 24 h after exposure either to alpha particles, neutrons, gamma rays, or X-rays. These results suggest that genetic insults are caused by ionizing radiation via not only ROS but also by other non-random mechanisms irrespective of the quality of radiation. We are now undertaking a study of 4934del in tissues from patients injected with Thorotrast to confirm its relevance to long-term radiation exposure. Exposure to alpha particles and low doses of neutrons induced 4934del, suggesting that high Linear Energy Transfer (LET) radiation is more effective than low LET radiation in inducing mtDNA deletions. We need further study to confirm whether this assumption is correct or not, and understand the similarity in mechanism between different qualities of radiation.

In conclusion, CD is induced after exposure to radiation irrespective of the quality of radiation. Cells with CD selectively died within 10 days of exposure. The novel mtDNA deletion found in this study could be useful as a marker of radiation damage irrespective of the quality of radiation.

Acknowledgements

This study was supported in part by Grants-in-Aid from the Ministry of Education, Science, Sports and Culture and the Ministry of Health, Labor and Welfare of Japan and in collaboration with Center for Interdisciplinary Research, Tohoku University.

References

Adema AD, Cloos J, Verheijen RH, Braakhuis BJ, Bryant PE. 2003. Comparison of bleomycin and radiation in the G2 assay of chromatid breaks. International Journal of Radiation Biology 79(8):655–661.

Anderson S, Bankier AT, Barrell BG, de Bruijn MH, Coulson AR, Drouin J, Eperon IC, Nierlich DP, Roe BA, Sanger F, Schreier PH, Smith AJ, Staden R, Young IG. 1981. Sequence and organization of the human mitochondrial genome. Nature 290(5806):457–465.

Berneburg M, Grether-Beck S, Kurten V, Ruzicka T, Briviba K, Sies H, Krutmann J. 1999. Singlet oxygen mediates the UVA-induced generation of the photoaging-associated mitochondrial common deletion. The Journal of Biological Chemistry 274(22):15345–15349.

Brooks AL. 2005. Paradigm shifts in radiation biology: their impact on intervention for radiation-induced disease. Radiation Research 164(4 Pt 2):454–461.

Brown WM, George M Jr, Wilson AC. 1979. Rapid evolution of animal mitochondrial DNA. Proceedings of the National Academy of Sciences of the USA 76(4):1967–1971.

Coffey G, Lakshmipathy U, Campbell C. 1999. Mammalian mitochondrial extracts possess DNA end-binding activity. Nucleic Acids Research 27(16):3348–3354.

Fukumoto M, Kuwahara Y, Ohkubo Y, Wang L. 2006. Analysis of carcinogenic mechanisms of liver cancers induced by chronic exposure to alpha-particles from internally deposited Thorotrast. Radiation Measurement 41:1186–1190.

Holt IJ, Harding AE, Morgan-Hughes JA. 1989. Deletions of muscle mitochondrial DNA in mitochondrial myopathies: sequence analysis and possible mechanisms. Nucleic Acids Research 17(12):4465–4469.

Jou MJ, Peng TI, Wu HY, Wei YH. 2005. Enhanced generation of mitochondrial reactive oxygen species in cybrids containing 4977-bp mitochondrial DNA deletion. Annals of the New York Academy of Sciences 1042:221–228.

Kubota N, Hayashi J, Inada T, Iwamura Y. 1997. Induction of a particular deletion in mitochondrial DNA by X rays depends on the inherent radiosensitivity of the cells. Radiation Research 148(4):395–398.

Lakshmipathy U, Campbell C. 1999. Double strand break rejoining by mammalian mitochondrial extracts. Nucleic Acids Research 27(4):1198–1204.

Morales CT, Atencio DP, Oca-Cossio J, Diaz F. 2003. Techniques and pitfalls in the detection of pathogenic mitochondrial DNA mutations. Journal of Molecular Diagnostics 5:197–208.

Paul R, Dalibart R, Lemoine S, Lestienne P. 2001. Expression of *E. coli* RecA targeted to mitochondria of human cells. Mutation Research 486:11–19.

Petros JA, Baumann AK, Ruiz-Pesini E, Amin MB, Sun CQ, Hall J, Lim S, Issa MM, Flanders WD, Hosseini SH, Marshall FF, Wallace DC. 2005. MtDNA mutations increase tumorigenicity in prostate cancer. Proceedings of the National Academy of Sciences of the USA 102(3):719–724.

Prithivirajsingh S, Story MD, Bergh SA, Geara FB, Ang KK, Ismail SM, Stevens CW, Buchholz TA, Brock WA. 2004. Accumulation of the common mitochondrial DNA deletion induced by ionizing radiation. FEBS Letters 571(1–3):227–232.

Ratain MJ. 2001. Pharmacology of cancer chemotherapy. In: DeVita VT Jr, Hellman S, Rosenberg SA, editors. Cancer principles and practice of oncology. 6th ed. Philadelphia, PA: Lippincott Williams & Wilkins. pp 335–459.

Samuels DC, Schon EA, Chinnery PF. 2004. Two direct repeats cause most human mtDNA deletions. Trends in Genetics 20(9):393–398.

Sankaranarayanan K. 1991. Ionizing radiation and genetic risks. III. Nature of spontaneous and radiation-induced mutations in mammalian *in vitro* systems and mechanisms of induction of mutations by radiation. Mutation Research 258(1):75–97.

Satoh M, Kuroiwa T. 1991. Organization of multiple nucleoids and DNA molecules in mitochondria of a human cell. Experimental Cell Research 196(1):137–140.

Schoeler S, Szibor R, Gellerich FN, Wartmann T, Mawrin C, Dietzmann K, Kirches E. 2005. Mitochondrial DNA deletions sensitize cells to apoptosis at low heteroplasmy levels. Biochemical Biophysical Research Communications 332(1):43–49.

Schon EA, Rizzuto R, Moraes CT, Nakase H, Zeviani M, DiMauro S. 1989. A direct repeat is a hotspot for large-scale deletion of human mitochondrial DNA. Science 244(4902):346–349.

Suzuki K, Ojima M, Kodama S, Watanabe M. 2003. Radiation-induced DNA damage and delayed induced genomic instability. Oncogene 22(45):6988–6993.

Wang XF, Simpkins JW, Dykens JA, Cammarata PR. 2002. Oxidative damage to human lens epithelial cells in culture: Estrogen protection of mitochondrial potential, ATP, and cell viability. Investigative Ophthalmology & Visual Science 44(5):2067–2075.

J. Radiat. Res., 48, 39–44 (2007)

Regular Paper

Oxidative Stress Induced Lipocalin 2 Gene Expression: Addressing its Expression under the Harmful Conditions

Mehryar Habibi ROUDKENAR[1,2], Yoshikazu KUWAHARA[1], Taisuke BABA[1], Amaneh Mohammadi ROUSHANDEH[3], Shigeko EBISHIMA[1], Shinya ABE[4], Yasuhito OHKUBO[4] and Manabu FUKUMOTO[1]*

Lipocalin 2/H_2O_2/oxidative stress/radiation/liver.

Lipocalin 2 (Lcn2, NGAL) is a member of the lipocalin superfamily with diverse functions such as the transport of fatty acids and the induction of apoptosis. Previous reports indicated that expression of *Lcn2* is induced under harmful conditions. However, the mechanisms of the induction of *Lcn2* expression remain to be elucidated. In this report, we intended to identify the factor or factors that induce *Lcn2* expression. Up-regulation of *Lcn2* expression after X-ray exposure was detected in the heart, the kidney and especially in the liver. Primary culture of liver component cells revealed that this up-regulation in the liver was induced in hepatocytes. Up-regulation of *Lcn2* expression was also detected in HepG2 cells after the administration of X-rays or H_2O_2. Interestingly, up-regulation of *Lcn2* expression after H_2O_2 treatment was canceled by the addition of the anti-oxidants, dimethylsulfoxide or cysteamine. These results strongly suggest that *Lcn2* expression is induced by reactive oxygen species. Therefore, Lcn2 could be a useful biomarker to identify oxidative stress both *in vitro* and *in vivo*.

INTRODUCTION

The lipocalins constitute a broad but evolutionally conserved family of small proteins. Although the primary function of the lipocalins is thought to be involved in the transport of small ligands such as fatty acids and pheromones, they have also been implicated in a variety of different functions such as retinol transport, cryptic coloration, olfaction, prostaglandin synthesis, regulation of the immune response and cell homeostatic mediation.[1)] Neutrophil gelatinase-associated lipocalin (NGAL, lipocalin 2, Lcn2) is a 25 kDa glycoprotein that was initially purified from neutrophil granules.[2)] The Lcn2 protein exists as a 25 kDa monomer, as a 46 kDa homodimer, and in a covalent complex with neutrophil gelatinase that is known as matrix metalloproteinase 9.[2)] A variety of functions of the Lcn2 protein have been reported, such as the transport of fatty acids and iron,[3–4)] the induction of apoptosis,[5)] the suppression of bacterial growth,[6)] and the modulation of inflammatory responses.[7)] The expression of the *Lcn2* gene is detected in mouse fibroblasts stimulated by a number of growth factors such as serum, basic fibroblast growth factor and phorbol esters. *Lcn2* expression is also observed in the mouse liver after treatment with some carcinogens or reactive oxygen species (ROS) producing agents such as diethylnitrosamine.[8)] These findings suggest that the Lcn2 protein may play a role in regulating cellular growth. This hypothesis is further supported by the expression of the Lcn2 protein in various malignant tumors.[9–11)] Contrary to previous reports, most functions of the Lcn2 protein, with the exception of its role in innate immunity, are not verified in *Lcn2* deficient mice.[12)] Another member of the lipocalin family, human tear lipocalin (Lcn1), acts as an oxidative-stress induced scavenger of potentially harmful products.[13)] In spite of the fact that there is little similarity between the Lcn1 and the Lcn2 proteins, they commonly exhibit antimicrobial activity.[6,14)] Several reports indicated that *Lcn2* expression is induced in various cells under harmful conditions such as cancer, intoxication, infection, inflammation, kidney injury, heart injury and burn injury where production of free radicals has been reported.[9–11,15–19)] Our previous study revealed that *Lcn2* expression was induced in the mouse liver when exposed to alpha particles (Roudkenar *et al.*, manuscript submitted). It has also been

*Corresponding author: Phone: +81-22-717-8507,
Fax: +81-22-717-8507,
E-mail: fukumoto@idac.tohoku.ac.jp
[1]Department of Pathology, Institute of Development, Aging and Cancer, Tohoku University, 4-1 Seiryo-machi, Aoba-ku, Sendai 980-8575, Japan; [2]Research Center, Iranian Blood Transfusion Organization, Tehran, Iran; [3]Department of Anatomy, Medicine Faculty, Medical University of Tabriz, Tabriz, Iran; [4]Department of Radiopharmacy, Tohoku Pharmaceutical University, 4-4-1 Komatsushima, Aoba-ku, Sendai 981-8558, Japan.
doi:10.1269/jrr.06057

reported that *Lcn2* expression was up-regulated in some radio-resistant cell lines established by continuous fractionated exposure to X-rays.[20] From the above results we hypothesized that *Lcn2* expression is induced by ROS. In this study we examined *Lcn2* expression in mouse tissues and HepG2 cells after irradiation. We also examined *Lcn2* expression after the administration of H_2O_2 and its scavengers.

MATERIALS AND METHODS

Mice

Seven-week old male C3H/Hex mice were used. Animal protocols were approved by the ethical committee of the Institute of Development, Aging and Cancer (IDAC), Tohoku University, and were performed according to the institutional guidelines.

Cell culture

HepG2 cells derived from human hepatoblastoma were obtained from the Cell Resource Center for Biomedical Research in IDAC, Tohoku University. Cells were maintained in RPMI-1640 medium (Sigma, St. Louis, MO, USA) supplemented with 10% fetal bovine serum (FBS; Invitrogen, Carlsbad, CA, USA). Cell cultures were raised at 37°C in an atmosphere of 5% CO_2.

H_2O_2 treatment

Before H_2O_2 treatment, HepG2 cells were cultured in serum-free medium for 16 hrs. After washing with phosphate buffered saline (PBS), cells were cultured in serum-free medium containing 0.1 mM H_2O_2 for 45 min. For scavenger treatments we also added 1 mM cysteamin or 5% dimethyl sulfoxide (DMSO; Sigma) to the H_2O_2 containing medium.

Irradiation

Mice were exposed to 2, 5 or 8.5 Gy of ^{60}Co γ-rays (0.34 Gy/min) at the Research Reactor Institute, Kyoto University. Liver, lungs, heart, spleen, testis and kidneys were dissected out from mice after sacrificed by cervical dislocation. All tissues were immediately frozen and kept at –80°C until use. HepG2 cells and mice for the isolation of parenchymal cells (hepatocytes, PC) and non-parenchymal cells (NPC) were exposed to 8.5 Gy X-rays (1.0 Gy/min.) using a 150-KVp X-rays generator (Model MBR-1520R, Hitachi, Tokyo, Japan) with a total filtration of 0.5 mm aluminum plus 0.1 mm copper filter. Long-term irradiated HepG2 cells were exposed to 0.5 Gy X-rays every 12 hrs for more than 4 years, and the total exposure dose was over 1,600 Gy.

Assessment of Lcn2 *gene expression*

Total RNA from mouse tissues and cells were extracted using Trizol reagent (Invitrogen) according to the manufacturer's protocol. Reverse transcription (RT) was performed by SuperScript III reverse transcriptase (Invitrogen) with 500 ng of *DNaseI* (Invitrogen) treated total RNA. Polymerase chain reaction (PCR) was performed using Animal *Taq* DNA polymerase (ABgene, Surrey, UK) in a GeneAmp PCR system 9600 (PerkinElmer Life and Analytical Sciences, Inc., Wellesley, MA, USA). After initial denaturation (5 min at 94°C), complementary DNA was subjected to 30 cycles of PCR. Primers for the amplification of mouse *Lcn2* were; forward 5'-CCA GTT CGC CAT GGT ATT TTT C-

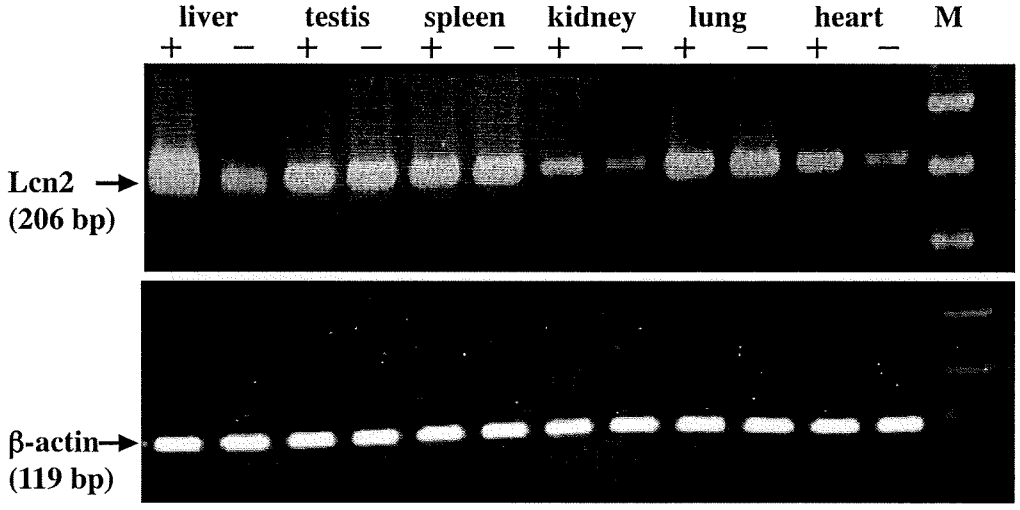

Fig. 1. Expression of *Lcn2* in mouse organs with or without exposure to γ-rays. Twenty-four hrs after exposure to 8.5 Gy of γ-rays *Lcn2* expression was determined by semi-quantitative RT- PCR. *Lcn2* expression was detected in all the organs examined before irradiation. After γ-ray irradiation *Lcn2* expression was up-regulated in the liver, the kidney and the heart. M; 100 bp marker. +; with γ-rays. –; without γ-rays.

3' and reverse 5'- CAC ACT CAC CAC CCA TTC AGT T-3'. Primers for human *Lcn2* were; forward 5'-TCA CCT CCG TCC TGT TTA GG-3' and reverse 5'-CGA AGT CAG CTC CTT GGT TC-3'. Gene expressions were normalized by *β-actin* expression and primers were; forward 5'-TTC TAC AAT GAG CTG CGT GTG G -3' and reverse 5'-GTG TTG AAG GTC TCA AAC ATG AT-3'. PCR annealing temperature was 60°C for human and mouse *Lcn2* and 59°C for *β-actin*. PCR products were separated in a 2% agarose gel. In order to determine gene expression, real-time PCR was performed in a BIO-RAD icycler iQ, SA-THK Real-Time PCR system (Bio-Rad Laboratories, Hercules, CA, USA). Amplification was conducted using AB solute SYBR green ROX mix (ABgene) according to the manufacture's instructions. The PCR conditions were; initial denaturation at 96°C for 15 min followed by 40 amplification cycles consisting of denaturation at 96°C for 30 sec, annealing at a suitable temperature for 30 sec and extension at 72°C for 30 sec. Threshold cycle values were normalized by *β-actin* expression.

Isolation of parenchymal cells (PC) and non-parenchymal cells (NPC)

PC and NPC were isolated from mouse liver tissue as described elsewhere.[21] Briefly, 24 hrs after exposure to 8.5 Gy of X-rays, mice were anaesthetized with pentobarbital (Dainippon Sumitomo Pharma, Co., Ltd., Osaka, Japan) followed by cannulation of the portal vein with a 24-gauge needle. Then, the liver was perfused with prewarmed calcium-free Hank's Balanced Salt Solution (HBSS, Sigma), at a flow rate of 3 ml/min. Subsequently, the liver was perfused with collagenase solution (Wako Pure Chemical Industries, Ltd., Osaka, Japan; 0.5 mg/ml HBSS containing 5 mM calcium) for 7 min. Liver component cells were gently isolated and were maintained in HBSS. Differential centrifugations were used to separate PC from NPC. The PC fraction was separated from total cells by centrifugation for 2 min at 50*g* and the pellet was washed three times with HBSS. Viability of isolated cells was assessed by the trypan blue dye exclusion test immediately after isolation and was found to be more than 70%. For separation of the NPC fraction, the cell suspension was centrifuged twice for 5 min at 50*g* to eliminate PC. Subsequently, the NPC fraction was sedimented by centrifugation of supernatant for 10 min at 150*g*.

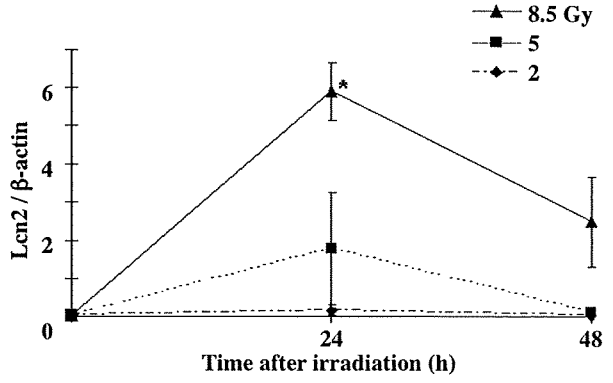

Fig. 2. Real-time PCR analysis of *Lcn2* expression in the mouse liver after exposure to γ-rays. Dose dependent up-regulation of *Lcn2* expression was observed 24 hrs after irradiation. (Mean ± SD, *; $p < 0.001$)

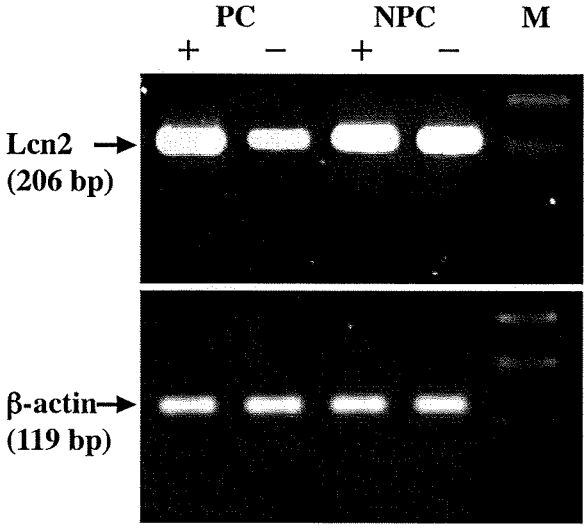

Fig. 3. Up-regulation of *Lcn2* expression in PC after exposure to 8.5 Gy of X-rays. PC and NPC were separately obtained from the irradiated mouse liver by perfusion. PC; parenchymal cells. NPC; non-parenchymal cells. M; 100 bp marker. +; with X-rays. –; without X-rays.

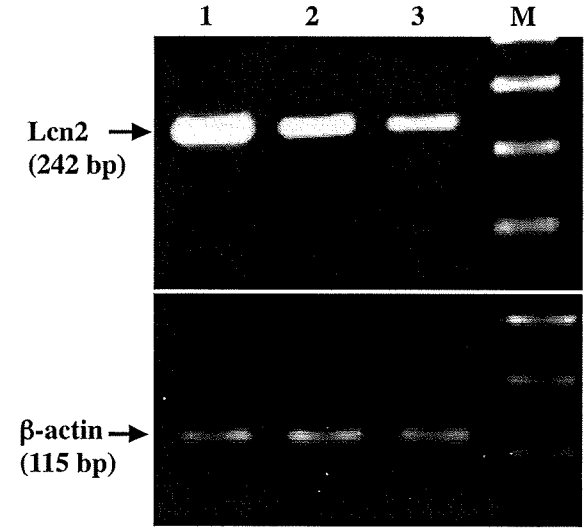

Fig. 4. Up-regulation of *Lcn2* expression after acute or long-term X-ray irradiation. Total RNA was extracted from HepG2 cells and *Lcn2* expression was examined by semi-quantitative RT-PCR. Lane 1; Long-term X-rays. Lane 2; 8.5 Gy of X-rays. Lane 3; without X-rays. M; 100 bp marker.

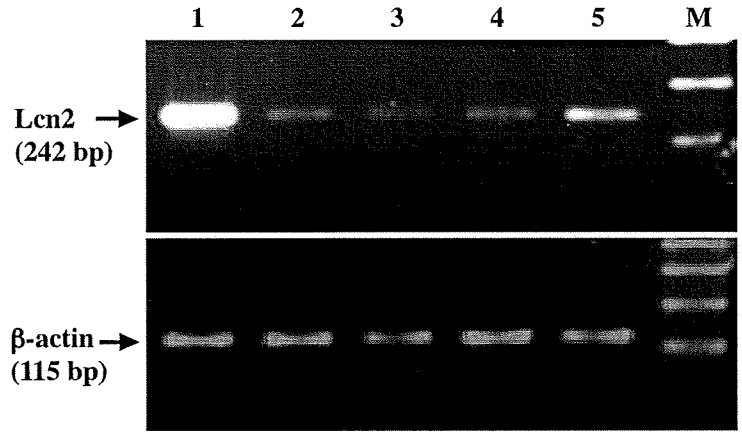

Fig. 5. Up-regulation of *Lcn2* expression after treatment with H_2O_2. Up-regulation of *Lcn2* expression was induced by the administration of H_2O_2. This up-regulation was suppressed by the addition of 5% DMSO or 1 mM cysteamine in the medium containing H_2O_2. Lane 1; 0.1 mM H_2O_2. Lane 2; 0.1 mM H_2O_2 and 1 mM cysteamine. Lane 3; 0.1 mM H_2O_2 and 5% DMSO. Lane 4; serum-free medium. Lane 5; No treatment. M; 100 bp marker.

Statistical analysis

The results were expressed as the mean ± SD of three independent experiments. Differences between groups were compared using the Student's *t*-test.

RESULTS

Lcn2 *expressions in mouse tissues after exposure to γ-rays*

We examined the effect of γ-rays on *Lcn2* expression by semi-quantitative RT-PCR. Before irradiation, *Lcn2* expression was detected in all the organs examined (Fig. 1). Twenty-four hrs after exposure to 8.5 Gy of γ-rays, *Lcn2* expression was up-regulated in the kidney, the heart and especially in the liver (Fig. 1). We then quantified *Lcn2* expression in the irradiated liver by real-time PCR (Fig. 2). Up-regulation of *Lcn2* expression was dose dependent and statistical significance was detected in the 8.5 Gy exposed group compared to non-irradiated mice ($p < 0.001$). In order to identify which compartment of the liver expressed *Lcn2*, we separated mouse liver cells into PC and NPC by the perfusion sedimentation technique. PC and NPC fraction mainly contained hepatocytes and Kupffer cells, respectively. Basal level of *Lcn2* expression in NPC was higher than that in PC (Fig. 3). After 8.5 Gy X-rays administration, up-regulation of *Lcn2* expression was detected in PC but not in NPC (Fig. 3).

Induction of Lcn2 expression in HepG2 cells after acute and long-term X-rays exposure

Since the liver was the most sensitive organ for the induction of *Lcn2* after irradiation (Fig. 1), we examined *Lcn2* expression *in vitro* using HepG2 cells. Up-regulation of *Lcn2* expression was detected 12 hrs after exposure to 8.5 Gy of X-rays (Fig. 4). *Lcn2* expression level in cells with long-term fractionated irradiation was higher than in cells after an acute exposure (Fig. 4).

Induction of Lcn2 *expression after H_2O_2 treatment*

The effect of ROS on *Lcn2* expression was examined by treating HepG2 cells with H_2O_2. Before H_2O_2 treatment, HepG2 cells were cultured in serum-free RPMI-1640 medium to avoid any influence of external free radicals such as lipid peroxidation products or antioxidants present in the serum. Without serum, *Lcn2* expression decreased, however, the administration of H_2O_2 drastically up-regulated *Lcn2* expression (Fig. 5). With the presence of 5% DMSO or 0.1 mM cysteamine in the H_2O_2 containing medium, up-regulation of *Lcn2* expression was canceled (Fig. 5).

DISCUSSION

Several studies indicate that *Lcn2* expression is induced under harmful conditions such as intoxication, infection, inflammation or other forms of cellular stresses,[8–11,15–19] however, the reason for the induction remains to be elucidated. Previous reports indicated that expression of *Lcn1*, a member of the lipocalin superfamily, was induced by harmful products such as ROS under conditions such as kidney injury, heart failure and burn injury.[15–19] Therefore, we hypothesized that harmful products such as ROS also induce *Lcn2* expression. To confirm our assumption, we examined *Lcn2* expression after the administration of H_2O_2 and also after Ionizing Radiation (IR), that is also a potent inducer of ROS.[22–23]

Without irradiation, *Lcn2* expression was detected in all the mouse organs examined. The Lcn2 protein in the testis

is known to be involved in protection of spermatogenic cells from genotoxic stresses such as ROS, and high expression of the *Lcn2* protein in the lung might be necessary to cope with the high level of ROS produced in this organ.[24] In this study, drastic up-regulation of *Lcn2* expression induced by IR was detected in the liver. Previous reports indicated that hepatocyte growth factor (HGF) induced by IR subsequently induces *Lcn2* expression.[25] HGF expression is reportedly induced under the condition of renal tubular injury, heart and liver diseases[26–28] accompanied with the production of ROS and induction of the *Lcn2* gene expression.[15–19] Therefore, high level of *Lcn2* expression in the irradiated liver might be due to the HGF induced by ROS. However, there is no report which indicates that ROS induces HGF expression. The up-regulation of *Lcn2* expression in the irradiated mouse liver may be attributed to both HGF and ROS. A previous report indicated that HGF is produced in Kupffer cells and endothelial cells.[29] Therefore, we further studied *Lcn2* expression after separating liver cells into PC and NPC. Basal level of *Lcn2* expression in NPC was higher than that in PC presumably because ROS are endogenously produced in Kupffer cells for the mediators in antigen presentation.[30] In this study, IR induced *Lcn2* upregulation in PC but not in NPC. It is noted that ROS are prominently produced in hepatocytes, but not in Kupffer cells after the administration of toxic injury.[31] These suggest that *Lcn2* expression in the irradiated liver is attribute to ROS produced in PC.

After acute and long-term exposure to X-rays, *Lcn2* expression was found to be upregulated in HepG2 cells. The level of up-regulation after long-term exposure to X-rays was higher than that after single acute exposure. This is consistent with the previous result using esophageal cancer cell lines.[20] In the present study, H_2O_2 induced up-regulated *Lcn2* expression in HepG2 cells and this up-regulation was canceled by the administration of ROS scavengers. Thus, we confirmed that *Lcn2* up-regulation in the liver is induced via ROS produced by IR. It is suggested that the Lcn2 protein might have a function as a scavenger and protect cells from ROS. The study to confirm these assumptions is now underway in our laboratory. This study also suggested that Lcn2 could be a useful biomarker for the detection of oxidative stress *in vitro* and *in vivo*.

ACKNOWLEDGMENTS

We thank all the members of Fukumoto's laboratory.

REFERENCES

1. Flower, D. R. (1993) The lipocalin protein family: structure and function. Biochem. J. **318**: 1–14.
2. Triebel, S., Blaser, J., Reinke, H., Tschesche, H. (1992) A 25 kDa alpha 2-microglobulinrelated protein is a component of the 125 kDa form of human gelatinase. FEBS. Lett. **314**: 386–388.
3. Chu, S. T., Lin, H. J., Huang, H. L., Chen, Y. H. (1998) The hydrophobic pocket of 24p3 protein from mouse uterine luminal fluid: fatty acid and retinol binding activity and predicted structural similarity to lipocalins. J. Pept. Res. **52**: 390–397.
4. Yang, J., Goetz, D., Li, J. Y., Wang, W., Mori, K., Setlik, D., Du, T., Erdjument-Bromage, H., Tempst, P., Strong, R., Barasch, J. (2002) An iron delivery pathway mediated by a lipocalin. Mol. Cell. **10**: 1045–1056.
5. Devireddy, L. R., Teodoro, J. G., Richard, F. A., Green, M. R. (2001) Induction of apoptosis by a secreted lipocalin that is transcriptionally regulated by IL-3 deprivation. Science. **293**: 829–834.
6. Goetz, D. H., Holmes, M. A., Borregaard, N., Bluhm, M. E., Raymond, K. N., Strong, R. K. (2002) The neutrophil lipocalin NGAL is a bacteriostatic agent that interferes with siderophoremediated iron acquisition. Mol. Cell. **10**: 1033–1043.
7. Cowland, J. B., Borregaard, N. (1997) Molecular characterization and pattern of tissue expression of the gene for neutrophil gelatinase-associated lipocalin from humans. Genomics. **45**: 17–23.
8. Kirstin, M., Ju-Seog, L., Patricia, A. D., Wen-Qing, C. M., Sambasiva, R., Snorri, S. T., Janardan, K. R. (2003) Molecular profiling of hepatocellular carcinomas developing spontaneously in acyl-CoA oxidase deficient mice: comparison with liver tumors induced in wild-type mice by a peroxisome proliferator and a genotoxic carcinogen. Carcinogenesis. **24**: 975–984.
9. Fried, A., Stoesz, S. P., Buckley, P., Gould, M. N. (1999) Neutrophil gelatinaseassociated lipocalin in normal and neoplastic human tissues. Cell type-specific pattern of expression. Histochem. J. **31**: 433–441.
10. Nielsen, B. S., Borregaard, N., Bundgaard, J. R., Timshel, S., Sehested, M., Kjeldsen, L. (1996) Induction of NGAL synthesis in epithelial cells of human colorectal neoplasia and inflammatory bowel diseases. Gut. **38**: 414–420.
11. Missiaglia, E., Blaveri, E., Terris, B., Wang, Y. H., Costello, E., Neoptolemos, J. P., Crnogorac-Jurcevic, T., Lemoine, N. R. (2004) Analysis of gene expression in cancer cell lines identifies candidate markers for pancreatic tumorigenesis and metastasis. Int. J. Cancer. **112**: 100–112.
12. Thorsten, B., Atsushi, T., Gordon, S. D., Andrew, J. E., Annick, Y. T., Andrew, W., Hannah, E. H., Carol, C. C., Tak, W. M. (2006) Lipocalin 2-deficient mice exhibit increased sensitivity to Escherichia coli infection but not to ischemia-reperfusion injury. Proc. Natl. Acad. Sci. USA. **7**: 1834–1839.
13. Markus, L., Petra, W., Bernhard, R. (2001) Human tear lipocalin acts as an oxidative- stressinduced scavenger of potentially harmful lipid peroxidation products in a cell culture system. Biochem. J. **356**: 129–135.
14. Maria, F., Hubertus, H., Petra, M., Ben, J. G., Bernhard, R. (2004) Human Tear Lipocalin exhibits antimicrobial activity by scavenging microbial siderophores. Antimicrob. Agents Chemother. **48**: 3367–3372.
15. Jaya, M., Kiyoshi, M., Qing, M., Caitlin, K., Jonathan, B., Prasad, D. (2004) Neutrophil gelatinase-associated lipocalin: a novel early urinary biomarker for cisplatin nephrotoxicity. Am. J. Nephrol. **24**: 307–315.

16. Jaya, M., Qing, M., Caitlin, K., Mark, M., Prasad, D. (2006) Kidney NGAL is a novel early marker of acute injury following transplantation. Pediatr. Nephrol. **21**: 856–863.
17. Frank, J. G. (2005) Oxygen, oxidative stress, hypoxia, and heart failure. J. Clin. Invest. **115**: 500–508.
18. Hemdahl, A. L., Gabrielsen, A., Zhu, C., Eriksson, P., Hedin, U., Kastrup, J., Thoren, P., Hansson, G. K. (2006) Expression of neutrophil gelatinase-associated lipocalin in atherosclerosis and myocardial infarction. Arterioscler. Thromb. Vasc. Biol. **26**: 136–142.
19. Vemula, M., Berthiaume, F., Jayaraman A., Yarmush, M. L. (2004) Expression profiling analysis of the metabolic and inflammatory changes following burn injury in rats. Physiol. Genomics. **18**: 87–98.
20. Fukuda, K., Sakakura, C., Miyagawa, K., Kuriu, Y., S Kin, Y., Nakase, A., Hagiwara, S.; Mitsufuji, Y., Okazaki, Y. H., Yamagishi, H. (2004) Differential gene expression profiles of radioresistant oesophageal cancer cell lines established by continuous fractionated irradiation. British. J. Cancer. **91**: 1543–1550.
21. Auger, A., Truong, T. Q., Rhainds, D., Lapointe, J., Letarte, F., Brissette, L. (2001) Low and high density lipoprotein metabolism in primary cultures of hepatic cells from normal and apolipoprotein E knockout mice. Eur. J. Biochem. **268**: 2322–2330.
22. Riley, P. A. (1994) Free radicals in biology: oxidative stress and the effects of ionizing radiation. Int. J. Radiat. Biol. **65**: 27–33.
23. Miura, Y. (2004) Oxidative stress, radiation-adaptive responses, and aging. J. Radiat. Res. **45**: 357–372.
24. Jennifer, L. T., Funmei, Y., Michael, D. G., Claude, A. P., Andrew, J. G. (2004) The iron cycle and oxidative stress in the lung. Free. Radic. Biol. Med. **36**: 850–857.
25. Gwira, J. A., Wei, F., Ishibe, S., Ueland, J. M., Barasch, J., Cantley, L. G. (2005) Expression of neutrophil gelatinase-associated lipocalin regulates epithelial morphogenesis in vitro. J. Biol. Chem. **280**: 7875–7882.
26. Liu, Y. (2002) Hepatocyte growth factor and the kidney. Curr. Opin. Nephrol. Hypertens. **11**: 23–30.
27. Ueno, S., Ikeda, U., Hojo, Y., Arakawa, H., Nonaka, M., Yamamoto, K., Shimada, K. (2001) Serum hepatocyte growth factor levels are increased in patients with congestive heart failure. J. Card. Fail. **7**: 329–334.
28. Okano, J., Shiota, G., Kawasaki, H. (1999) Expression of hepatocyte growth factor (HGF) and HGF receptor (c-met) proteins in liver diseases: an immunohistochemical study. Liver. **19**: 151–159.
29. Noji, S., Tashiro, K., Koyama, E., Nohno, T., Ohyama, K., Taniguchi, S., Nakamura, T. (1990) Expression of hepatocyte growth factor gene in endothelial and Kupffer cells of damaged rat livers, as revealed by in situ hybridization. Biochem. Biophys. Res. Commun. **173**: 42–47.
30. Maemura, K., Zheng, Q., Wada, T., Ozaki, M., Takao, S., Aikou, T., Bulkley, G. B., Klein, A. S., Sun, Z. (2005) Reactive oxygen species are essential mediators in antigen presentation by Kupffer cells. Immunol Cell Biol. **83**: 336–343.
31. Loguercio, C., Federico, A. (2003) Oxidative stress in viral and alcoholic hepatitis. Free. Radic. Biol. Med. **34**: 1–10.

Received on July 27, 2006
Revision received on September 28, 2006
Accepted on October 3, 2006
J-STAGE Advance Publication Date: January 16, 2007

J. Radiat. Res., 49, 29–40 (2008)

Regular Paper

Gene Expression Profiles in Mouse Liver Cells after Exposure to Different Types of Radiation

Mehryar Habibi ROUDKENAR[1,2], Li LI[1], Taisuke BABA[1], Yoshikazu KUWAHARA[1], Hironobu NAKAGAWA[1], Lu WANG[1], Satoshi KASAOKA[3], Yasuhito OHKUBO[4], Koji ONO[5] and Manabu FUKUMOTO[1]*

Gene expression/Microarray/Mouse liver/Radiation quality/Endothelial cell/Kupffer cell.

The liver is one of the target organs of radiation-induced cancers by internal exposures. In order to elucidate radiation-induced liver cancers including Thorotrast, we present a new approach to investigate *in vivo* effects of internal exposure to α-particles. Adopting boron neutron capture, we separately irradiated Kupffer cells and endothelial cells in mouse liver *in vivo* and analyzed the changes in gene transcriptions by an oligonucleotide microarray. Differential expression was defined as more than 3-fold for up-regulation and less than 1/3 for under-regulation, compared with non-irradiated controls. Of 6,050 genes examined, 68 showed differential expression compared with non-irradiated mice. Real-time polymerase chain reaction validated the results of the microarray analysis. Exposure to α-particles and γ-rays produced different patterns of altered gene expression. Gene expression profiles revealed that the liver was in an inflammatory state characterized by up-regulation of positive acute phase protein genes, irrespective of the target cells exposed to radiation. In comparison with chemical and biological hepatotoxicants, inductions of Metallothionein 1 and Hemopexin, and suppressions of cytochrome P450s are characteristic of radiation exposure. Anti-inflammatory treatment could be helpful for the prevention and protection of radiation-induced hepatic injury.

INTRODUCTION

The biological effects of exposure to high linear energy transfer (LET) radiation have a particular relevance to radiation protection and risk assessment. Although internal exposure to high LET radiation is of a major concern, it is characterized by the existence of target organs and the difficulty of dose estimation. Thorotrast, a colloidal suspension of radioactive $^{232}ThO_2$ that naturally emits α-particles, was used as a radiographic contrast agent in the 1930s–1950s. More than half of intravasculary injected Thorotrast deposited in the liver caused liver cancers decades after the injection because of its life-long deposition and exposure to α-particles. Our histological examination of the liver from 144 cases of Thorotrast patients revealed intrahepatic cholangiocellular carcinoma (ICC, 25.7%), angiosarcoma (AS, 20.8%), hepatocellular carcinoma (HCC, 14.6%) and combined tumors (2.1%). Considering that Japan is an endemic area of hepatitis virus B and C, and that HCC comprises more than 80% of liver cancers, ICC and AS may be considered to be characteristic of Thorotrast-induced liver tumors. Our previous study showed that injected Thorotrast is phagocytosed by macrophages and radioactive Thorium is always migrating within the affected livers via Thorotrast-laden macrophages. These suggest that the liver is evenly exposed to α-particles at the organ level despite the short range of α-particles.[1)] Internal deposition of plutonium also causes chronic exposure to high levels of α-particles with increased risk of liver cancers including AS.[2)] Neither the deposited amount of Thorium nor the incubation period from injection to tumor induction is significantly different between cases with ICC and AS (manuscript in preparation). Consequently we thought that cell-to-cell interaction between irradiated macrophages and/or epithelial cells and parenchymal cells of the liver is involved in the development of ICC while direct irradiation of endothelial cells of the

*Corresponding author: Phone: +81-22-717-8507,
Fax: +81-22-717-8512,
E-mail: fukumoto@idac.tohoku.ac.jp
[1]Department of Pathology, Institute of Development, Aging and Cancer, Tohoku University, Sendai 980-8575, Japan; [2]Research Center, Iranian Blood Transfusion Organization Tehran, Iran; [3]Faculty of Pharmaceutical Sciences, Hiroshima International University, Hiroshima 737-0112, Japan; [4]Department of Radiopharmacology, Tohoku Pharmaceutical University, Sendai 981-8558, Japan; and [5]Radiation Oncology Research Laboratory, Research Reactor Institute, Kyoto University, Osaka 590-0494, Japan.
doi:10.1269/jrr.07078

sinusoid is the principal contributor to the development of AS. A few studies also have been shown that exposure to α-particles induces liver tumors in mouse and other rodents.[3,4]

Thermal neutrons cause the boron atom to split into an α-particle and a lithium nucleus via the boron neutron capture reaction (BNC). Both of these particles have a very short range (about one cellular diameter) and cause significant damage to the cell in which boron atoms are located. BNC therapy (BNCT) adopts this cytotoxic effect by selective delivery of boron-10 (^{10}B) to tumor cells: the short range nature of the effects of BNC minimizes the damage to adjacent normal cells. A large amount of ^{10}B compound can be administered in a liposome-incorporated form, which is then phagocytosed by macrophages. Conjugation of the liposome with polyethylene glycol (PEG) is known to increase blood levels of ^{10}B compounds and reduced uptake by macrophages.[5] Recent radiological studies focus on the molecular mechanisms underlying transcriptional responses of mammalian cells to ionizing radiation. It is now apparent that the cellular reactions to ionizing radiation are complex and involve the activation of secondary messenger pathways and increased transcription of immediate early response genes.[6]

These observations prompted us to adopt BNC to investigate *in vivo* effects of internal radiation exposure to α-particles. In this study, we prepared the ^{10}B-liposome treatment and the ^{10}B PEG-liposome treatment to expose Kupffer cells and endothelial cells to α-particles respectively, and analyzed the changes of gene expression using a microarray containing probes for 6,050 genes. As well as elucidation of the biological relevance of radiation, the present study also

Table 1. Primer sets for RT-PCR

Symbol	GenBank		Sequence	Size(bp)
AK3	AK005194	forward reverse	5'-GTG TGT TGG CCA AGA CTT TC-3' 5'-ATG TAT CCA GCG AGC AGT AAG-3'	236
Atp5b	AK010314	forward reverse	5'-GCA CAA TGC AGG AAA GGA TCA C-3' 5'-ACG TCA TAA TGC TCA TTG CCA AC-3'	241
ATP5c1	AK007063	forward reverse	5'-CGC CCC ATG GCA ACT CTG AAA G-3' 5'-GCC AAA GAA CCT GTC CCA TAC A-3'	160
Brap	AK013885	forward reverse	5'-AAA GGG CTG AAG TGC TGA ATC-3' 5'-TCT GGC GTT TGA CAG TAT CGG C-3'	211
Car3	AK003671	forward reverse	5'-CTT GAT GCC CTG GAC AAA AT-3' 5'-AGC TCA CAG TCA TGG GCT CT-3'	180
Egfr	AK004944	forward reverse	5'-TGA GCA ACA TGT CAA TGG ACT TAC-3' 5'-GCA TGT GGC CTC ATC TTG GAA C-3'	263
Galnt3	AK019995	forward reverse	5'-CAC TAT TTA CCC GGA AGC GTA TG-3' 5'-GTG GCA CGT GTA CAG AAT CAA TG-3'	139
Gsta3	AK014076	forward reverse	5'-TGA CCT GGC AAG GTT ACG AAG TG-3' 5'-CAT TAT CTC CAG ATC CGC CAC TC-3'	199
Hpxn	BB610094	forward reverse	5'-ATC TCA GCG AG GTG GAA GAA TC-3' 5'-CCT TCA CTC TGG CAC TCT CCA C-3'	215
Lcn2	AK002932	forward reverse	5'-CCA GTT CGC CAT GGT ATT TTT C-3' 5'-CAC ACT CAC CAC CCA TTC AGT T-3'	206
Mt1	AK018727	forward reverse	5'-ACC TCC TTG CAA GAA GAG CTG CT-3' 5'-GCT GGG TTG GTC CGA TAC TAT T-3'	160
Mt2	AK002567	forward reverse	5'-GGG TCC CCA CAT CTG TG TAA-3' 5'-CAA CGG CTT TTA TTG TCA GTT AC-3'	115
β-actin		forward reverse	5'-TTC TAC AAT GAG CTG CGT GTG G-3' 5'-GTG TTG GAA GGT CTC AAA CAT GAT-3'	110

contributes to the understanding of general idea of potential target molecules for cancer therapy.

MATERIALS AND METHODS

Mice and radiation

Male C3H/Hex mice (6 weeks old) were exposed to whole-body irradiation. For irradiation of mice by α-particles, specifically to macrophages and endothelial cells, ^{10}B-liposomes and polyethylene glycol (PEG)-^{10}B-liposomes were respectively administered. There were two mice analyzed by microarray, independently treated, and five mice by real time PCR. Mice used for these 2 assays were from 2 different courses of experiments. The ^{10}B compound sodium mercaptoundecahydrododecaborate (BSH) was used.[7] Each compound was suspended in physiological saline at a concentration of 4,000 ppm and 100 μl of ^{10}B-liposome solution and 300 μl of PEG-^{10}B-liposome solution were injected via the tail vein. Four hours (hrs) after the administration, the mice were exposed to neutron radiation at the Research Reactor Institute, Kyoto University (RRIKU). Before the irradiation experiments for gene expression, the neutron fluence was monitored by radioactivation of gold foils in the front and back of the mouse container. The average fluence of the thermal neutron source was 2.1×10^{12} n/cm^2 and the average flux was 2.3×10^9 n/cm^2/s at 5 MW. The boron concentration of the liver was measured by γ-ray spectrometry using a thermal neutron guide. We determined the exposure period at the calculated dose of 8.5 Gy at an organ level. For control irradiation, the mice were exposed to the neutron source for the same period as the BNC group. The contribution of neutrons and γ-rays to the total exposure was 4.2 cGy and 33 cGy, respectively. As a control for the quality of radiation, the mice were exposed to γ-rays at a dose of 8.5 Gy (0.34 Gy/min) with a ^{60}Co γ-ray source. Twenty hrs after irradiation, the mice were sacrificed by cervical dislocation. The dissected liver was immediately frozen and stored at –80°C until use. Animal experiments were approved by the Ethical Committee of the Institute of Development, Aging and Cancer, Tohoku University and were performed in accordance with institutional guidelines.

Oligonucletide microarrays

In accordance with 'Functional Annotation of Mouse' for the RIKEN full-length cDNA clone (http://fantom2.gsc.riken.go.jp/) and GenBank (http://www.ncbi.nih.gov/Genbank), 6,050 mouse genes were chosen for microarray analysis. These consisted of genes associated with signal transduction (766), cancer (506), autoimmune/inflammatory disease (455), cytokine/inflammatory response (267), stem cell

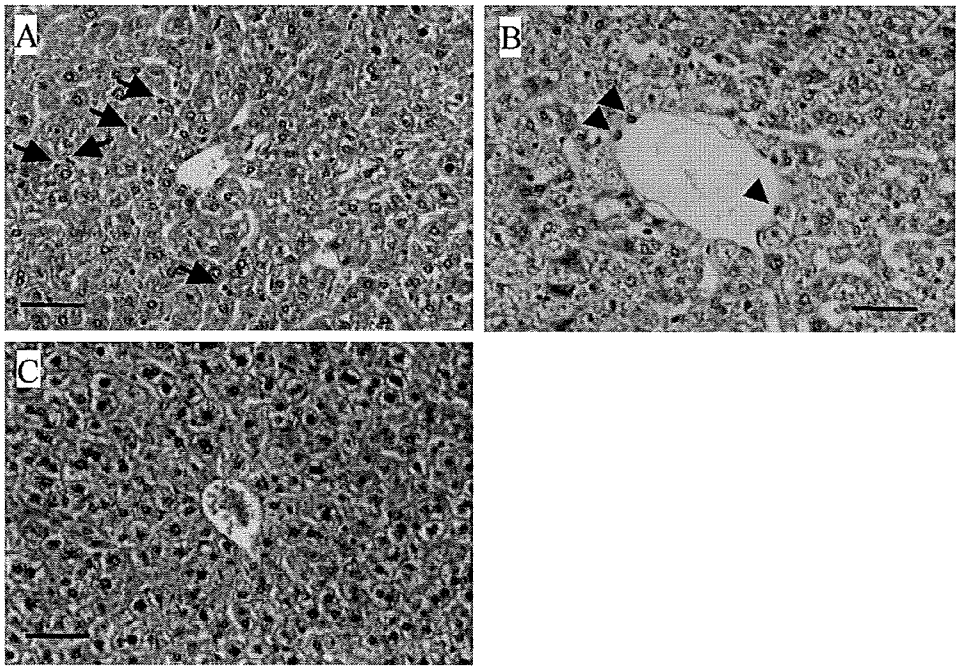

Fig. 1. Histological findings of the mouse liver following irradiation of Kupffer or endothelial cells. A: Compared with non-irradiated control, mice injected with ^{10}B-liposome solution showed a slight increase of the number and the size of Kupffer cells (arrows), indicating Kupffer cells were mainly irradiated (Kupffer exposure). B: Endothelial cells (arrow heads) were swollen in irradiated liver. The dilatation of sinusoids was noticed in mice injected with PEG-^{10}B-liposome, indicating sinusoidal endothelial cells were mainly insulted (Endothelial exposure). C: Non-irradiated control. Scale Bar: 50 μm.

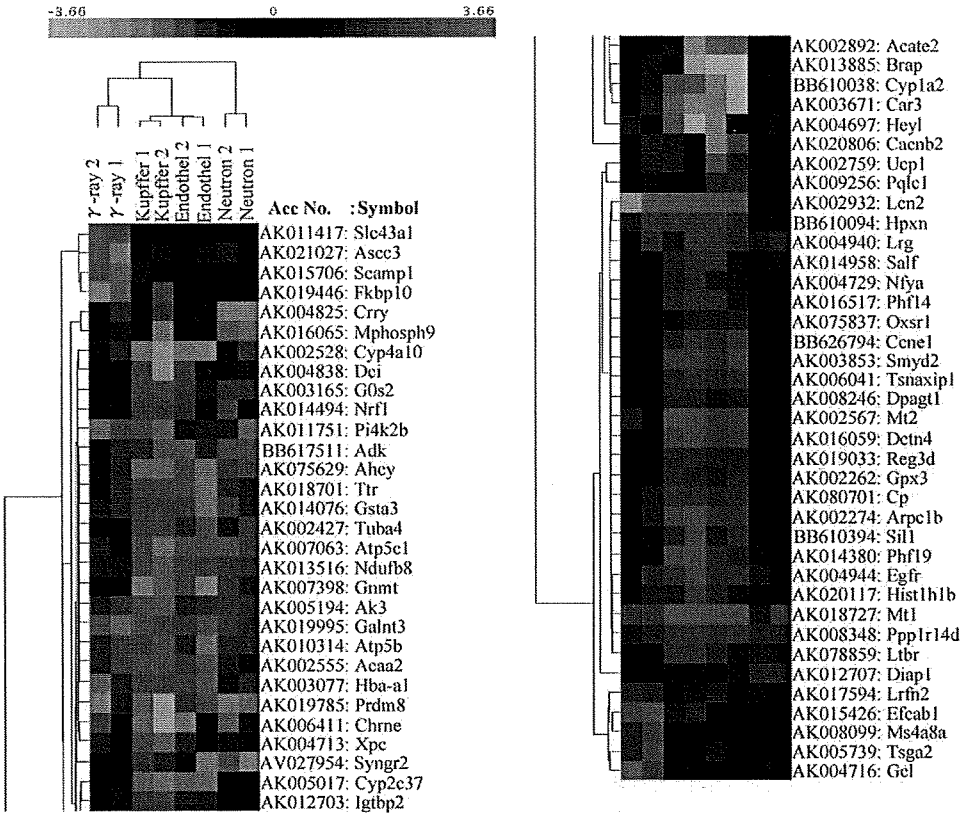

Fig. 2. Cluster analysis of individual mice according to the profile of gene expression examined. Mice from the same exposure group was the closest and the neutron exposure group was the most different from other groups.

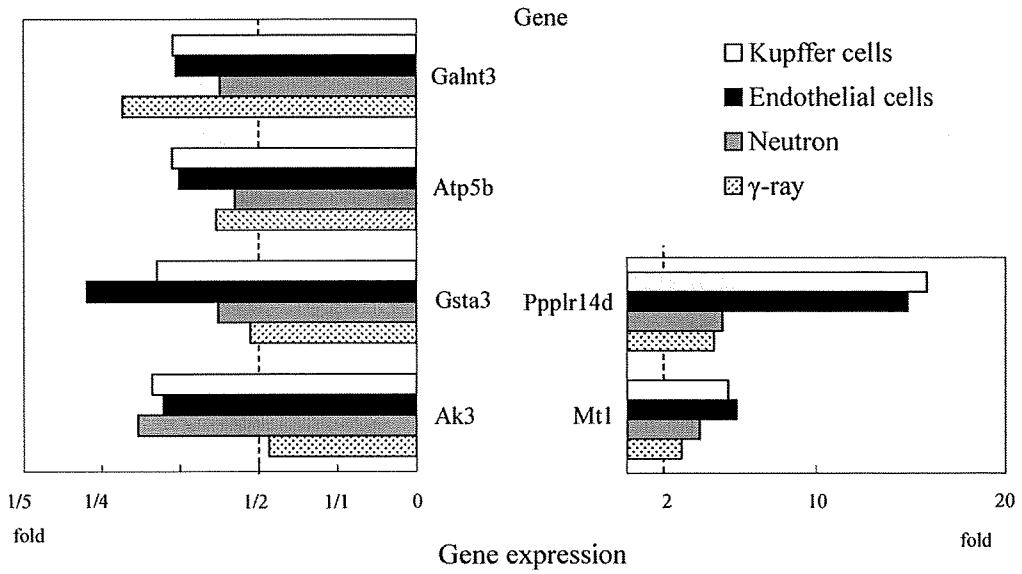

Fig. 3. Genes which are commonly over-expressed more than 2-fold or under-expressed less than a half following irradiation compared to control gene expression levels. Ak3: Adenylate kinase 3α, Gsta3: Glutathione S-transferase 3α, Atp5b: ATP synthase β subunit, Galnt3: UDP-N-acetyl-α-D-galactosamine-polypeptide, Mt1: Metallothionein 1, Ppp1r14d: Protein phosphatase 1, regulatory (inhibitor) subunit 14D.

(261), apoptosis (260), cardiovascular disease (240), neuroscience (197), toxicology/pharmacology (184), extracellular matrix/adhesion molecules (105), diabetes/obesity (105), developmental/regenerative disorder (102), cell cycle (99), and others (2,503).

After total RNA was extracted from the liver using TRIZOL reagent (Invitrogen Corp., Carlsbad, CA), Poly-A RNA was separated using dT(25)-coupled magnetic beads (Dynal Biotech, Oslo, Norway). Individual mice were evaluated for the change in gene expression against pooled liver RNA

Table 2-A. Up and down-regulated genes in all the irradiated groups

	Gene	Symbol	GenBank	Function
Up	Metallothionein 1	Mt1	AK018727	Metal binding
	Protein phosphatase 1, regulatory (inhibitor) subunit 14D	Ppp1r14d	AK008348	Protein phosphatase inhibitor
Down	Adenylate kinase 3α	Ak3	AK005194	Adenine metaboilsm
	Glutathione S-transferase α3	Gsta3	AK014076	Detoxication
	ATP synthase β subunit	Atp5b	AK010314	ATP synthesis
	UDP-N-acetyl-α-D-galactosamine-polypeptide	Galnt3	AK019995	Secretion

Table 2-B. Commonly up and down-regulated genes by Kupffer cell specific and endothelial cell specific exposures to α-particles

	Gene	Symbol	GenBank	Function
Up	Lipocalin 2	Lcn2	AK002932	Anti-apoptosis
	Metallothionein 2	Mt2	AK002567	Metal binding
	Actin related protein 2/3 complex, subunit 1B	Arpc1b	AK002274	Cytoskeleton, protein trafficking
	Dynactin 4	Dctn4	AK016059	Cytoskeleton, protein trafficking
	PHD finger protein 19	Phf19	AK014380	Chromatin regulation
	Epidermal growth factor receptor	Egfr	AK004944	Cell growth
	SET and MYND domain containing 2	Smyd2	AK003853	Transcription
	Endoplasmic reticulum chaperone SIL1 homolog	Sil1-pening	BB610394	Molecular chaperon
	Hemopexin	Hpxn	BB610094	Metal transporter, antioxidant
	Ceruloplasmin	Cp	AK080701	Metal transporter
	Cyclin E1	Ccne1	BB626794	Cell cycle
	Translin-associated factor X (Tsnax) interacting protein 1	Tsnaxip1	AK006041	Cell cycle
	Regenerating islet-derived δ	Reg3d	AK019033	Cell growth
	Glutathione peroxidase 3	Gpx3	AK002262	Antioxidant
Down	PR domain containing 8	Prdm8	AK019785	Chromatin regulation
	CYP4A10	Cyp4a10	AK002528	Metabolism
	S-adenosylhomocysteine hydrolase	Ahcy	AK075629	Adenosine metabolism
	Glycine N-methyltransferase	Gnmt	AK007398	Methylation
	CYP2C37	Cyp2c37	AK005017	Metabolism
	Carbonic anhydrase 3	Car3	AK003671	Antioxidant
	ATP synthase γ subunit	Atp5c1	AK007063	ATP synthesis
	NADH dehydrogenase (ubiquinone) 1β subcomplex 8	Ndufb8	AK013516	Electron transport
	Transthyretin	Ttr	AK018701	Negative acute phase protein
	CYP1A2	Cyp1a2	BB610038	Metabolism

Table 2-C. Up and down-regulated genes by Kupffer cell specific exposure to α-particles

	Gene	Symbol	GenBank	Function
Up	Lymphotoxin B receptor	Ltbr	AK078859	Immunity
	Histone 1, H1b	Hist1h1b	AK020117	Chromosome organization
	PHD finger protein 14	Phf14	AK016517	Chromatin regulation
	Stoned B/TFIIA- α/β -like factor	Salf	AK014958	Transcription factor, membrane traficking
	Nuclear transcription factor-Y α	Nfya	AK004729	Transcription factor
	UDP-GlcNAc:dolichyl-phosphate N-acetylglucosamine photransferase 1	Dpagt1	AK008246	Protein glycosylation
Down	Nicotinic cholinergic receptor, ε polypeptide	Chrne	AK006411	Neurotransmitter/receptor
	Hairy/enhancer-of-split related with YRPW motif	Heyl	AK004697	Transcriptioin repressor
	3,2 trans-enoyl-CoA isomerase	Dci	AK004838	b-Oxidation of unsaturated fatty acids
	Xeroderma pigmentosum, complementation group C	Xpc	AK004713	DNA repair
	G0/G1 switch gene 2	G0s2	AK003165	G0/G1 transition
	Tubulin, α 4	Tuba4	AK002427	Cytoskeleton
	Nuclear respiratory factor 1	Nrf1	AK014494	Transcription factor
	Acetyl-CoA-acyl transferase 2	Acaa2	AK002555	Fatty acid oxidation
	Insulin-like growth factor binding protein 2	Igfbp2	AK012703	Cell growth regulation

Table 2-D. Up and down-regulated genes by endothel specific exposure to α-particles

	Gene	Symbol	GenBank	Function
Up	Uncoupling protein 1	Ucp1	AK002759	Heat production
	Leucine-rich α-2-glycoprotein1	Lrg1	AK004940	Acute phase protein
	PQ loop repeat containing 1	Pqlc1	AK009256	Electron carrier
	Oxidative-stress responsive 1	Oxsr1	AK075837	Cytoskeleton
Down	BRCA1 associated protein	Brap	AK013885	DNA repair
	Voltage-dependent Ca channel (β2)	Cacnb2	AK020806	Ion channel
	Hemoglobin α adult chain 1	Hba-a1	AK003077	Oxygen delivery
	Acyl-CoA thioesterase 2	Acate2	AK002892	Signal trans., protein traffick

Table 2-E. Up and down-regulated genes by γ-ray exposure

	Gene	Symbol	GenBank	Function
Up	EF hand calcium binding domain 1	Efcab1	AK015426	Ca binding
	Germ cell-less homolog	Gcl	AK004716	Differentiation
	Testis specific gene A2	Tsga2	AK005739	Testis specific
	Membrane-spanning 4-domains, subfamily A, member 8A	Ms4a8a	AK008099	Transporter
	Leucine rich repeat and fibronectin type III domain containing 2	Lrfn2	AK017594	Cell adhesion signal trans.
Down	FK506 binding protein 10	Fkbp10	AK019446	Immunosuppression
	Activating signal cointegrator 1 complex subunit	Ascc3	AK021027	Transcription coactivator
	Secretory carrier membrane protein 1	Scamp1	AK015706	Endocytosis
	Solute carrier family 43, member 1	Slc43a1	AK011417	Transporter

Table 2-F. Up and down-regulated genes by neutron exposure

	Gene	Symbol	GenBank	Function
Up	Diaphanous homolog 1	Diap1	AK012707	Cytoskeleton
Down	Complement receptor related protein	Crry	AK004825	Immunity
	Synaptogyrin 2	Syngr2	AV027954	Synaptic transmission
	Phosphatidylinositol 4-kinase type 2 β	Pi4k2b	AK011751	Inositol lipid biosyhthesis
	M-phase phosphoprotein 9	Mphosph9	AK016065	Cell cycle
	Adenosine kinase	Adk	BB617511	Signal transduction

from the five control non-irradiated mice. Complementary DNA (cDNA) probes were generated starting with 1 μg of polyA RNA using a CyScribe First-Strand cDNA Labelling kit (Amersham Biosciences Corp., Piscataway, NJ). cDNA from irradiated mice was labeled with Cy5 and that from control mice was labeled with Cy3. Pre-hybridization and hybridization were carried out on UltraGAPS coated slides in accordance with the manufacturer's manual (Corning, NY). The image was captured in a GenePix 4000B (Axon Instruments, Inc. CA). The quantification of gene expression arrays was performed by Array Vision software (Imaging Research Inc., Ontario, Canada). Cluster analysis of gene expression was performed by the War method.[8] The experiments were carried out in independent duplicates.

Real-time PCR

In order to validate the results from the microarray analysis we selected 12 genes (Table 1) and compared their gene expression as measured by microarray analysis and real-time PCR. DNaseI treated 500 ng of total RNA was used for the synthesis of cDNA using superscript First-Strand Synthesis System (Invitrogen, Carlsbad, CA). cDNA corresponding to 10 ng of total RNA was amplified using Real-time PCR for the determination of gene expression using QuantiTect SYBR Green PCR Master Mix (QIAGEN K.K., Tokyo, Japan) in an iCycler (BIO-RAD, Hercules, CA). For the normalization of gene expression, a set of primers for β-actin was used.

RESULTS

Compared with non-irradiated controls, mice injected with ^{10}B-liposome solution showed a slight increase in the number and the size of Kupffer cells, indicating that Kupffer cells were irradiated (Kupffer exposure, Fig. 1A). The dilatation of sinusoids was noticed in mice injected with PEG-^{10}B-liposome, indicating sinusoidal endothelial cells were irradiated (Endothelial exposure, Fig. 1B). Liver tissues from mice exposed to γ-rays and neutrons revealed no remarkable histological changes (data not shown). In all cases, parenchymal hepatocytes did not show noticeable changes (Fig. 1).

Table 3. Comparison of gene expressioin levels between microarray and real-time PCR

Symbol	GenBank	endothelial			Kupffer			neutron			gamma		
		Real time-PCR	Micro-Array		Real time-PCR	Micro-Array		Real time-PCR	Micro-Array		Real time-PCR	Micro-Array	
		mean ± S.D.	Mouse 1	Mouse 2	mean ± S.D.	Mouse 1	Mouse 2	mean ± S.D.	Mouse 1	Mouse 2	mean ± S.D.	Mouse 1	Mouse 2
AK3	AK005194	0.66 ± 0.29	0.40	0.45	0.68 ± 0.10	0.29	0.27	0.84 ± 0.28	0.42	0.40	0.95 ± 0.33	0.38	0.48
Atp5b	AK010314	0.52 ± 0.06	0.22	0.44	0.72 ± 0.28	0.35	0.30	0.71 ± 0.17	0.43	0.44	0.90 ± 0.19	0.34	0.45
ATP5c1	AK007063	0.64 ± 0.06	0.27	0.26	0.68 ± 0.07	0.28	0.15	0.83 ± 0.29	0.33	0.28	1.47 ± 0.53	0.91	0.52
Brap	AK013885	0.69 ± 0.14	0.04	0.06	0.89 ± 0.32	0.94	0.13	1.23 ± 0.54	1.66	1.11	2.03 ± 0.71	0.62	0.97
Car3	AK003671	0.07 ± 0.053	0.04	0.20	0.14 ± 0.03	0.26	0.17	0.85 ± 0.27	1.14	1.09	0.53 ± 0.26	0.53	0.74
Egfr	AK004944	1.65 ± 0.84	5.41	4.90	3.39 ± 1.67	5.22	9.07	1.12 ± 0.69	1.68	2.81	1.93 ± 0.81	3.61	1.71
Galnt3	AK019995	0.19 ± 0.05	0.29	0.37	0.39 ± 0.20	0.30	0.34	0.68 ± 0.17	0.43	0.38	0.47 ± 0.06	0.24	0.30
Gsta3	AK014076	0.58 ± 0.14	0.18	0.30	0.85 ± 0.22	0.31	0.30	1.10 ± 0.21	0.46	0.34	0.67 ± 0.10	0.41	0.54
Hpxn	BB610094	36.53 ± 20.07	4.49	6.94	40.33 ± 17.23	6.42	6.38	2.56 ± 1.05	0.61	0.82	8.38 ± 5.3258	6.12	2.90
Lcn2	AK002932	1909.50 ± 558.5	94.79	95.38	1558.30 ± 133.6	34.90	62.41	1.94 ± 1.15	0.79	1.38	6.34 ± 5.20	128.21	–
Mt1	AK018727	24.22 ± 9.13	13.14	16.51	29.51 ± 8.88	15.35	16.38	1.67 ± 0.81	7.20	2.92	15.59 ± 10.66	5.12	4.11
Mt2	AK002567	38.46 ± 25.77	6.47	8.78	42.33 ± 7.71	12.84	19.36	2.57 ± 1.65	2.00	1.37	10.22 ± 7.43	1.99	3.32

Cluster analysis of the microarray results revealed that 2 mice from the same exposure group were the closest, indicating that all the experimental data in this study are reliable (Fig. 2). In this study, only the genes whose over-expression or under-expression compared with non-irradiated control levels which were consistently observed in 2 different mice with the same exposure levels were analyzed. In total, 161 genes were over-expressed by more than 2-fold and 32 genes

Table 4. Comparison of gene expression profiles between radiation exposures and hepatotoxicants

Gene	Symbol	GeneBank	Kupffer cells		Endothel		Neutrons		γ-rays		McMillian *et al.* (rat)	
			Mouse 1	Mouse 2	Mouse 1	Mouse 2	Mouse 1	Mouse 2	Mouse 1	Mouse 2	hepatotoxicants	PPA[a]
Macrophage activation/acute phase response												
Cytochrome P450, family 1, subfamily a, polypeptide 2	Cyp1a2	BB610038	0.32	0.30	0.07	0.15	1.47	1.07	0.63	0.89	0.51	
CYP2C37	Cyp2c37	AK005017	0.23	0.20	0.21	0.23	1.35	1.36	0.60	1.11	0.63	
Fatty acid binding protein 5, epidermal	Fabp5	AK011551	2.85	1.64	1.28	1.76	1.17	1.46	0.71	0.45	2.75	
G-6-phosphatase, transport protein 1	G6pt1	AK003620	0.45	0.43	0.54	0.58	0.70	0.55	0.87	1.39	0.51	0.46
Hemopexin	Hpxn	BB610094	6.41	6.38	4.49	6.94	0.61	0.82	6.12	2.90	1.57	
Insulin-like growth factor binding protein, acid labile subunit	Igfals	AK004926	–	–	–	–	0.32	0.64	1.18	0.52	0.41	
Latent TGF-β binding protein 1	Ltbp1	AK020449	0.41	0.01	0.73	0.08	1.05	0.25	–	0.42	1.06	0.84
Metallothionein 1	Mt1	AK018727	15.35	16.38	13.14	16.51	7.20	2.92	5.12	4.11	1.44	0.23
Pyruvate kinase, muscle	Pkm2	AK002341	1.10	1.23	1.19	1.48	1.00	1.31	1.26	–	2.41	
Retinol binding protein 4, plasma	Rbp4	AK004839	0.32	0.34	0.24	0.40	0.63	0.58	0.61	0.73	0.66	
Superoxide dismutase 2	Sod2	AK002534	1.73	1.77	2.34	1.45	0.76	0.46	1.09	0.96	2.69	
Peroxisome proliferator												
Acetyl-CoA dehydrogenase, medium chain	Acadm	AK008149	0.62	–	0.81	0.87	0.76	0.88	0.52	0.50	0.47	
Brain acyl-CoA hydrolase	Bach	AK010646	1.23	1.25	1.26	1.45	1.06	1.26	0.88	1.02	0.82	2.00
3-hydroxybutyrate dehydrogenase	Bdh	AK009575	0.59	0.66	0.67	0.83	0.76	0.57	0.75	0.54	0.38	
CD36 antigen	Cd36	AK004192	1.20	1.09	1.17	1.15	0.93	1.30	1.10	0.69	1.01	2.87
Dodecenoyl-CoA delta isomerase	Dci	AK004838	0.30	0.10	0.55	0.32	0.54	0.65	0.89	1.10	0.37	1.73
2,4-dienoyl CoA reductase 1	Decr1	AK004725	1.22	1.10	1.11	1.10	1.14	1.22	1.00	0.95	0.45	
Epoxide hydrolase 2	Ephx2	AK002415	0.54	0.55	0.62	0.50	0.99	0.89	0.82	0.75	0.28	
Fatty acid CoA ligase, long chain 2	Facl2	AK004897	0.39	0.32	0.37	0.38	0.68	0.76	0.60	0.73	0.34	
3-hydroxy-3-methylglutaryl-CoA synthase 2	Hmgcs2	AK004865	0.46	0.38	0.48	0.34	1.01	1.21	0.69	1.40	0.44	
ER stress/chaperone protein /HSP												
Annexin A2	Anxa2	AK012563	0.75	1.26	1.45	1.38	1.14	0.93	1.66	–	2.36	
Calreticulin	Calr	AK075605	1.58	1.57	1.35	1.88	0.62	1.21	1.79	1.13	2.28	0.65
Protein disulfide isomerase-related	Pdir	AK012415	1.38	1.35	1.18	0.60	0.94	1.15	0.88	0.58	2.14	0.62
Metabolism												
S-adenosylhomocysteine hydrolase	Ahcy	AK075629	0.21	0.18	0.14	0.26	0.30	0.35	0.42	0.64	0.41	
Betaine-homocysteine methyltransferase	Bhmt	AK016283	1.49	1.70	1.27	1.52	1.20	1.39	1.58	1.99	0.24	
Sulfotransferase family 1A, phenol-preferring, member 1	Sult1a1	AK002700	0.41	0.43	0.35	0.49	0.57	0.59	0.92	0.99	0.43	
Other functions												
G0/G1 switch gene 2	G0s2	AK003165	0.30	0.27	0.48	0.34	0.38	0.36	1.35	2.07	0.60	
Kininogen	Kng	AK005547	1.71	2.65	2.55	2.70	1.37	1.21	1.61	1.04	1.16	0.68
Solute carrier family 34 , member 2	Slc34a2	AK004832	0.45	0.23	0.81	1.78	0.74	1.18	1.24	1.37	1.06	1.59

Light gray background: Under-expressed genes; Black: Over -expressed genes
[a]: Peroxisome proliferator agonist